**Proceedings of ICFDP8:**
**8th Int. Congress of Fluid Dynamics & Propulsion**
**December 14-17,2006,Sharm El Shiekh, Sinai, Egypt.**

# ICFDP8-EG-140

# MEASUREMENTS OF FLOW OVER A MODEL OF A FINNED HIGH SPEED TRAIN

**I.K.Mohamed**
Higher Institute of Energy
South Valley University, Aswan, Egypt.

**Y.P.Kohama**
Institute of Fluid Science, Tohoku University, Sendai, Japan.

**A.S.Sabry**
Mechanical Engineering Department
Cairo University, Cairo, Egypt.

**M. A. Serag-Eldin**
Mechanical Engineering Department
American University in Cairo, Cairo, Egypt

## ABSTRACT

With the extensive increase of train speeds, the aerodynamics problems associated with the flows around such trains become increasingly important. In addition to stream-lining the surface of the train, it is found necessary to introduce fins in order to curb secondary vortices and improve flow characteristics.

The present work investigates experimentally the effect of introducing leading and trailing edge fins on the flow over a new model of a high speed train. The flow fields around such model were measured using both a PIV system and the X-Hotwire probe. In addition, the surface pressure distributions over the rear and front part of the train model were measured using a scan valve. The paper presents the results of the measurements together with the details of the experimental set-up and measurement techniques.

For both flows over the model of the Shinkansen series 300 and the new finned model, the measured data are analyzed and discussed. In addition to providing insight on the flow characteristics of high speed trains, the measurements are valuable for providing reference results necessary to validate computational models.

## INTRODUCTION

Aerodynamic and aeroacoustics problems that arise due to the increase of train speed are receiving at present a considerable attention and considered as practical engineering issues that need to be urgently solved.

In general, the train aerodynamics are related to aerodynamic drag, pressure variations inside the train, train-induced flows, cross wind effects, ground effects, pressure waves inside the tunnel, impulse waves at the exit of the tunnel, noise and vibration,….etc. The aerodynamic drag depends on the train shape, surface roughness of train body, and ground topography surrounding the traveling train [1]

For the train design as a whole, a drag coefficient reduction of 0.10 is estimated to be easily achievable [2]. If approximately 150 trains to be built, having an expected life time of 30 years, such a drag coefficient reduction would result in a saving of energy costs of about 16 million US$, which is about 50 times more than the costs spent for all the wind tunnel experiments [2].

In this study surface pressure, drag force and PIV are presented for both the Shinkansen series 300 and the new finned models. X-hotwire measurements are presented only for the modified model.

## NOMENCLATURE

| | |
|---|---|
| $C_d$ | Drag Coefficient |
| $C_l$ | Lift Coefficient |
| $C_p$ | Pressure Coefficient |
| D | Total Drag (kg f) |
| L | Train Nose Length (m) |
| L | Total Lift (Kg f) |
| N | Sample number in each record. |
| P | Local Surface Static Pressure (Pa) |
| Ps | Free Stream Static Pressure (Pa) |
| Re | Reynolds Number |
| Sa, Sb | Train Side Surface Pressure Lines |
| Ta, Tb, Tc | Train Top Surface Pressure Lines |
| U | The ensemble mean velocity (m/s) |

| | |
|---|---|
| V | velocity vector |
| X,Y,Z | Cartesian coordinates directions |

**GREEK LETTERS**

| | |
|---|---|
| ρ | fluid density |

**ABBREVIATIONS**

| | |
|---|---|
| M1 | New Train Model |
| M0 | Japanese Shinkansen Series 300 Model |
| PIV | Particle Image Velocity Meter |

## EXPERIMENTAL SETUP

The experiments were carried out in the low turbulence wind tunnel of the Institute of Fluid Science, Tohoku University, Sendai-Japan. The tunnel was constructed from steel, except from the inlet to the second diffuser to the end of the fourth corner, which was constructed of concrete since this part is situated outside the building.

The closed working section has an octagonal cross section of 1m in width and 3.5 m of length; the wind speed ranges from 5 to 70 m/s. The open-jet working section has an octagonal cross section of 1.42 m length with a 0.81 m width of diffuser exit and a wind speed range of 5~80 m/s [3].

The experiments were carried out in a circulating-type low turbulence wind tunnel with an open test section. Figure 1. shows the experimental setup and the coordinate system (X-axis was opposite the free stream direction; normal direction was Y-axis and spanwise direction was Z-axis; the axes origin was placed at the origin of the train nose for the X-Y plane and at the centerline of train body for the Z-Y plane).

Figure 2. shows a picture of the 1/30 scale train models for the two nose shapes, the new train shape (finned one) and the SHINKANSEN series 300 model shape. Figure 3. reveals the corresponding dimensions; both models have the same length (800 mm). The new train model (M1) has a nose length (250 mm) longer than the series 300 model (M0) (200 mm).

The strength of the compression wave in a tunnel strongly depends on the length of the train especially when the train is short [4]

M1-hydraulic diameter and cross-sectional area are 109 mm, and 10528.71 $mm^2$ respectively. M0 hydraulic diameter and cross-sectional area are 117 mm, 12275.42 $mm^2$ respectively. The ratio of the model area to that of the tunnel area (blockage ratio) should be less than 0.03 for a plate normal to the flow [5]. The M1 and M0 blockage ratio are 0.026 and 0.03 respectively.

The test in the low turbulence wind tunnel was carried out at 40 m/s ($Re_1$= $2.93x10^5$ and $Re_0$=$3.14x10^5$, i.e. a subcritical flow field) and Mach number of about 0.12 which allow incompressible flow calculations.

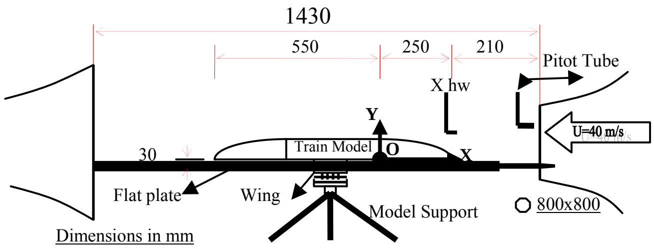


Figure 1. Wind tunnel experimental setup

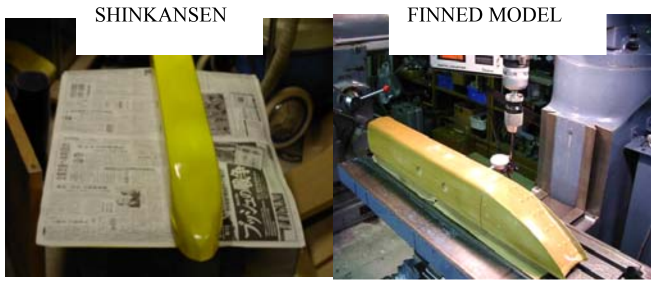


Figure 2. SHINKANSEN series 300 train model and new finned train model

### INSTRUMENTATION AND MEASURING TECHNIQUES

The instruments have been equipped with data acquisition, recording and processing facilities to measure the detailed velocity profiles using hot-wire anemometer, load cell to measure the drag force, scan valve to measure the surface pressure and Particle Image Velocity-meter PIV for flow visualization. Description, specification and techniques is given in [3].

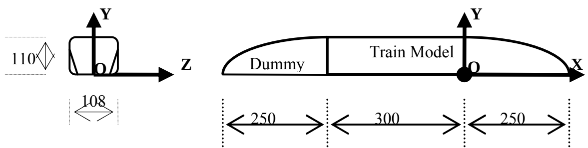


(a) M1

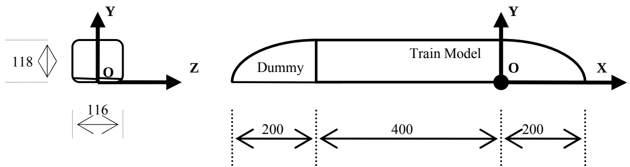


(b) M0

Figure 3. 1/30 scale train model dimensions in mm: (a) finned model. (b)SHINKANSEN series 300 model

The measuring technique means the adaptation of the instrument to match well with the conditions of the experiment, such that maximum accuracy and most reliable data can be obtained. Such technique includes selection of various control parameters of the measuring instrument, modification added to match the instrument with the experimental conditions and procedures to be followed during the experiments.

In a typical steady flow situation, it is conventional to decompose the instantaneous fluid velocity into turbulent fluctuation and mean velocity. The ensemble averaging technique may be employed. The ensemble mean velocity is defined as;

$$U = \frac{1}{N}\sum_{n=1}^{N}\tilde{U}(n)$$

Where N is the sample number in the record, and $\tilde{U}(n)$ is the velocity realization for the $n^{th}$ sample. It has the advantage of high accuracy due to the large number of samples.

The ensemble averaging technique was used to get the mean flow velocity and turbulence intensity distributions. The measurements were taken at many sections in different flow conditions (free flow, train front and train rear). Figure 4. shows the test sections coordinates.

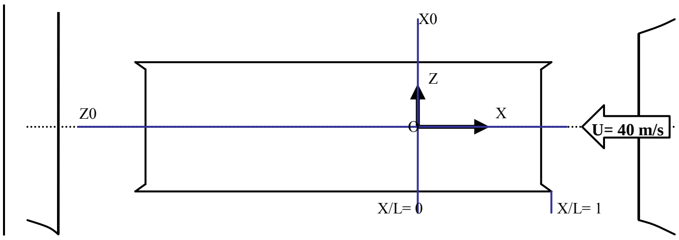


Figure 4. Experimental test sections coordinates

In the front region, ten test sections were measured from the symmetry plan and outward to the fin. PIV flow visualization for the front flow was not possible, so the flow velocity was measured in 35 test sections perpendicular to the mean flow direction. In the rear region, flow velocity was measured at 11 sections.

## RESULTS AND DISCUSSION

The measurements were performed for the 1/30 scale SHINKANSEN series 300 model M0 and new finned model M1.

### Surface Pressure Measurement

The train surface pressure measurements were conducted on one half of the train model nose. The surface pressure is lead to the model front by small tubes and measured by a mechanical pressure scan valve [6].

With the aid of Labview program and computer system, the steady pressure distribution is obtained. The surface pressure tap points position data were given to reference length which is the train model nose length, L.

The starting point is at X/L=0 and the ending point at X/L=1 for the front part. For the train model rear, the starting point is at X/L=0 and the ending point at X/L=-1.

The surface pressure points were distributed on the top (Ta, Tb and Tc) and on the side (Sa and Sb) of the train model nose. These points are shown in Figure 5.

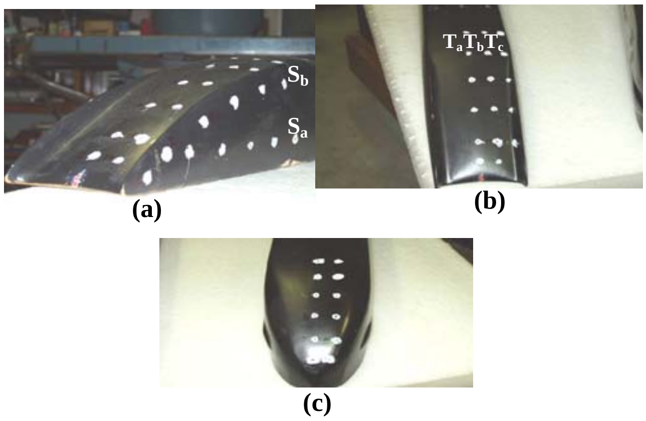


Figure 5. Surface pressure points locations; (a) and (b) for finned model and (c) for SHINKANSEN series 300 model

Figure 6. shows M0-M1 top surface pressure coefficient. The results indicate that the pressure coefficient for both models is almost the same in the front region and different in the rear region due to the wake characteristics. The pressure coefficient Cp is calculated from the following relation:

$$Cp = \frac{2(P - Ps)}{\rho V^2}$$

Where P = Local surface static pressure.
ρ = Air density.
Ps = Free stream static pressure.
V = Free stream velocity.

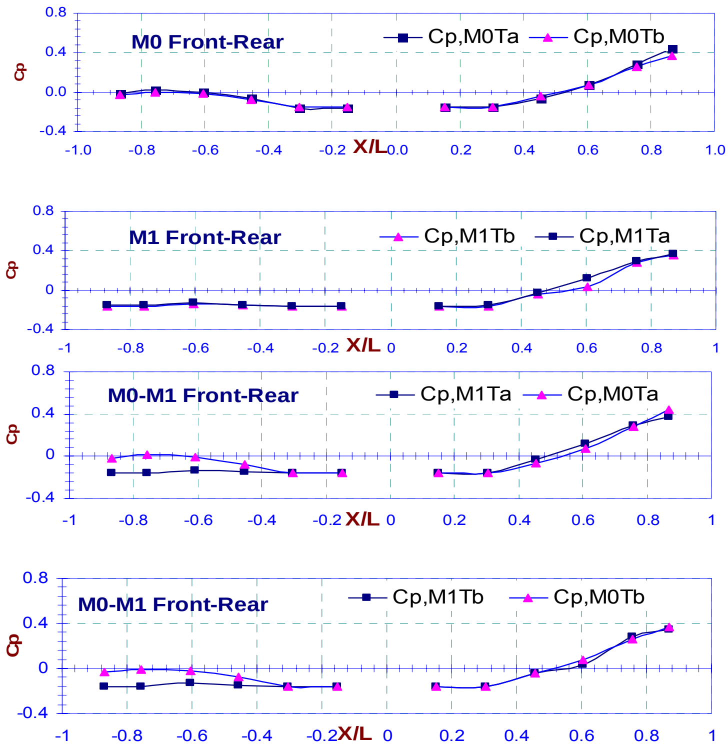


Figure 6. M0-M1 top surface pressure distribution at flow velocity 40 m/s

## Drag and Lift Measurements

Controlling drag force is the most important factor in the aerodynamic study of the high speed trains. In this study LMC-3501-50N load cell was used to measure the drag force for both models, M0 and M1.

Figure 7. shows the aerodynamic load comparison between both models M1 and M0 at different wind tunnel speed. The results indicate that the drag coefficient ($C_d$) for M1 is less than that of M0 whereas the lift coefficient ($C_l$) for M1 is higher than that of M0 indicating higher lift/drag ratio. At the train speed of 40 m/s, the drag coefficient was reduced by about 7% compared with that of M0, due to vortex guidance in the wake of M1.

It can be noticed from the figure that the drag coefficient slope decreases at high speed, indicating very small change in $C_d$.

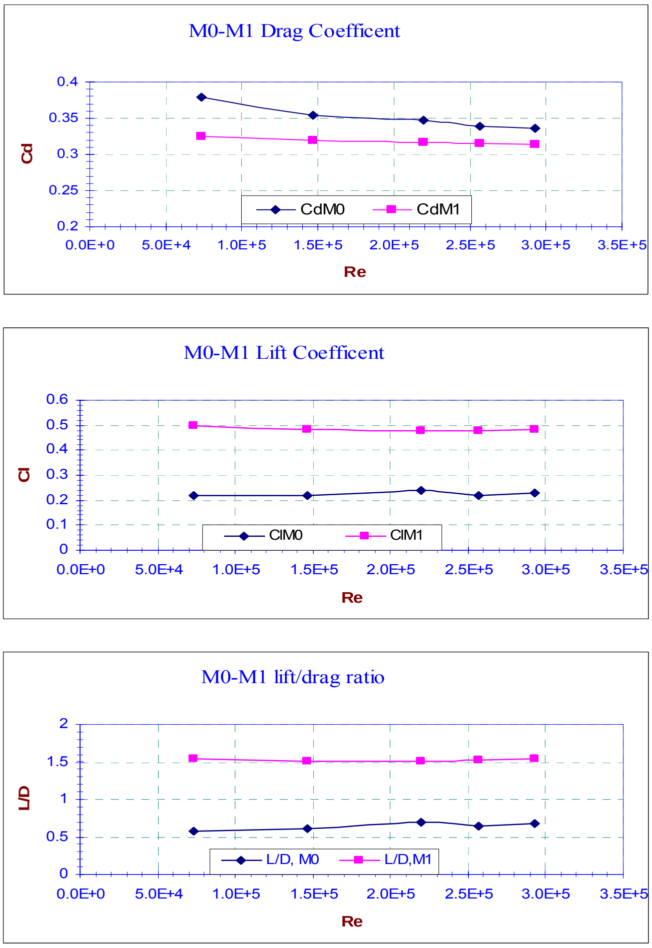


Figure 7. Aerodynamic load comparison between the New Train Model M1 and the SHINKANSEN Series 300 Model M0

## Flow Visualization

Since flow visualization is an effective tool to help understand the flow phenomena, a Particle Image Velociymetry (PIV) system with the data processing software, Insight 2, were used in the train model wake. X plane PIV data for both models in the rear area are shown in Figs. 8 at different X values. The first X-section was at -560 mm which is 10 mm behind the model trailing edge. The second X-section was at -700 mm which is relatively far from the model. The last section is -800 mm which is far away from the train trailing edge.

Figure 8. indicates the appearance of a strong non-homogenous vortex behind the SHINKANSEN series 300 trailing edge model (M0) which becomes weak away from the model.

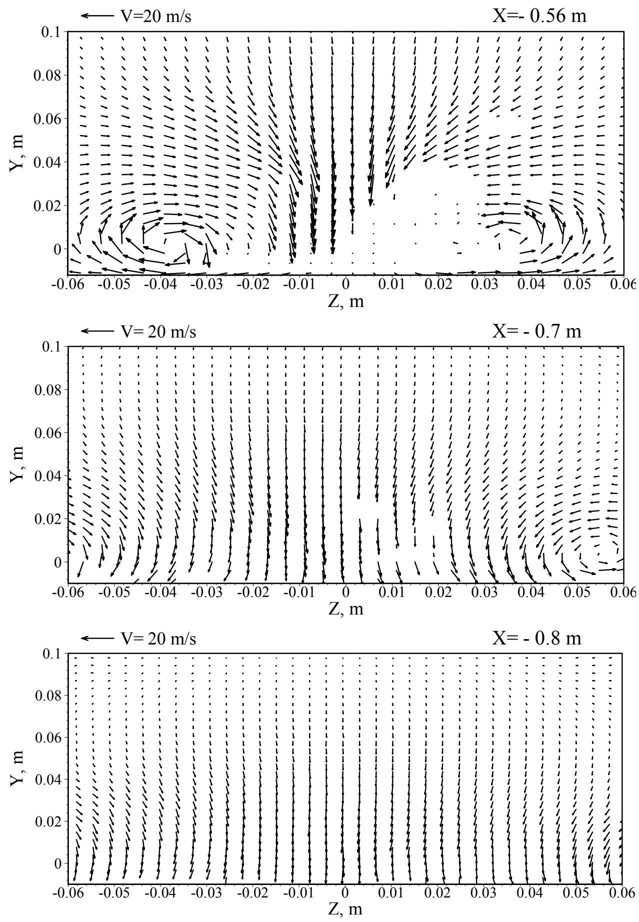


Figure 8. SHINKANSEN Series 300 Model Rear (M0)PIV data at 40 m/s flow velocity at different X values.

Figure 9. shows that the vortex behind the new finned trailing edge model (M1) is more homogeneous than that of the M0 model and becomes weak far away from the new finned trailing edge model.

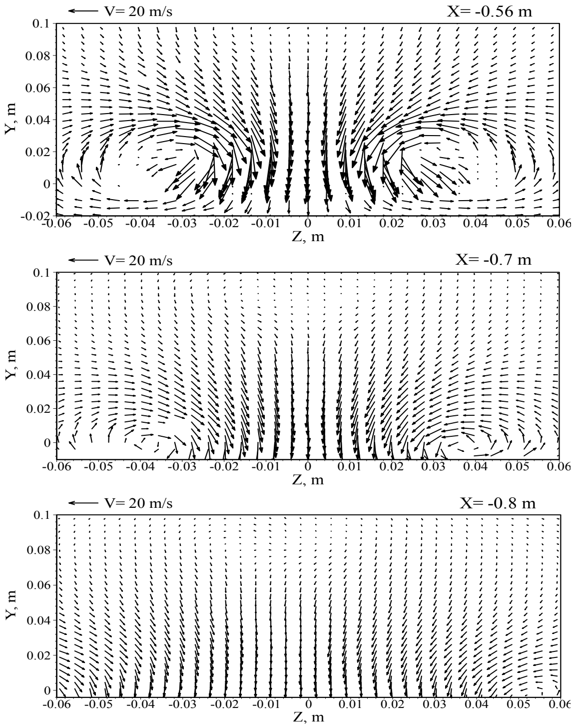


Figure 9. New Train Model Rear (M1) PIV data at 40 m/s flow velocity at different X values

a) M0

b) M1

Figure 10. Movie Capture for both models.

In order to appreciate the differences between the secondary vortices formed with and without fins, one should see the behavior of the vortices with time. This is available on a video film which shows clearly the attachment and stabilization of these vortices with fins. Two captures from this movie are shown in Fig. 10.

It can be concluded from the results that the new finned model (M1) has improved the wake characteristics of the SHINKANSEN series 300 model (M0), by guiding the vortices over and behind the train rear.

## Flow Velocity Measurement

Flow velocities were measured using X-Probe at 40 m/s free stream velocity. The flat plate measurements indicate that the boundary layer thickness is about 20 mm and the flow turbulence level at inlet section is about 0.2 % outside and about 5.5 % inside the boundary layer region [1].

In this study, the axial velocity component U for two X-Probes (one in the Z plane (UV) and the other in the Y plane (UW)) was measured. Figure 11 shows the change rate percentage of the axial velocity component U for both X-Probes, in which the velocity was measured at different X-planes; in upstream plane (X=410 mm) and in downstream planes (vortex region; X=-560 mm, X=-700 mm and X=-800 mm). The horizontal axis represents the measured points at different Y locations and the vertical axis is the difference between the axial velocity components for both X-Probes as a percentage of the UV X-Probe Value.

The results indicate that the error percentage of the axial component is relatively small in the uniform flow (upstream section). The error percentage is about 3 % of the axial component value, while the error percentage is relatively high in the wake region (downstream region). It reaches values between +11%:-47 just behind the train model at X=-560 mm. These high values decreased away from the train wake. The error percentage reaches values between +8%:-19% at X=-700 mm, while far away from the model, it reaches values between +6%:-7%.

It can be concluded that the X-Probe relatively accurate in the upstream region (uniform flow) and less accuarte in the downstream region (non-uniform flow due to the existence of vortices). Thus the X-Probe could only be accepted as a flow visualization tool in the vortices's regions.

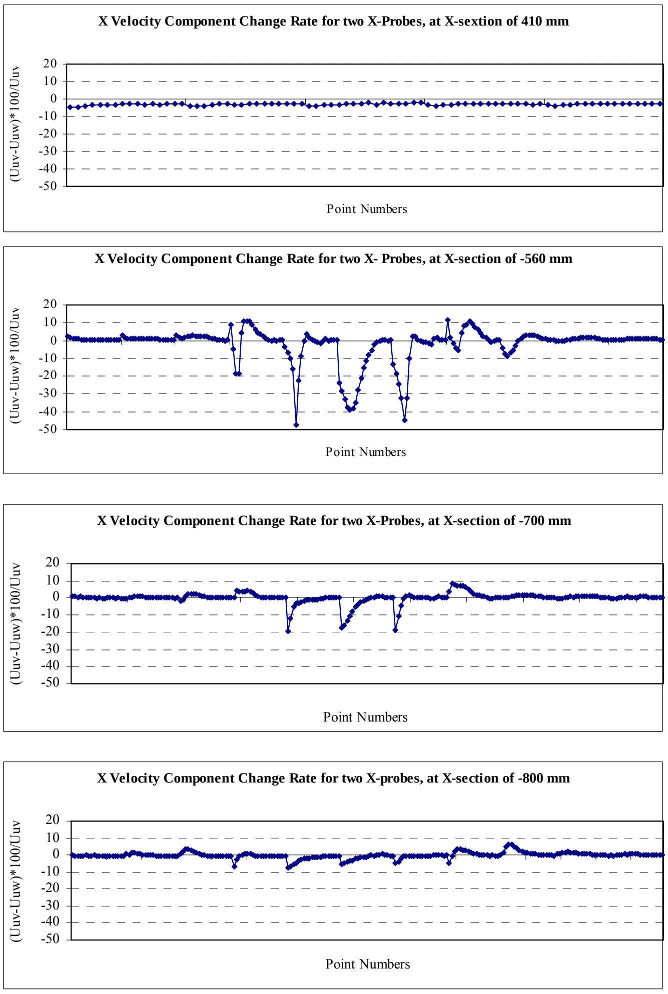


Figure. 11 Change Rate Percentage of X Velocity Component Data Measured by Two X-Probe (UV & UW) with New Model at Different X Values

Figure 12. shows the velocity vectors over the new train front model at different Z planes; symmetry plane Z0, edge plane Z40 and near model plane Z57. As shown in the figure, the measured velocity has a maximum value at the front head surface. The velocity vectors data indicate the flow convergence on the roof of the train.

Figure 13. shows the X-Probe velocity vectors over the new train front model at different X planes. The first X-section is 260 mm which is 10 mm in front of the leading edge of the new train model; the second and the third are crossing the new model nose, in which the vortex formation in the front region of the finned model is very clear near the edge.

Figure 14. shows the X-Probe velocity vectors over the new train model rear at different Z planes; symmetry plane Z0, edge plane Z40 and near model plane Z57. The results indicate smooth velocity distribution over the train body and high velocity values near the finned area.

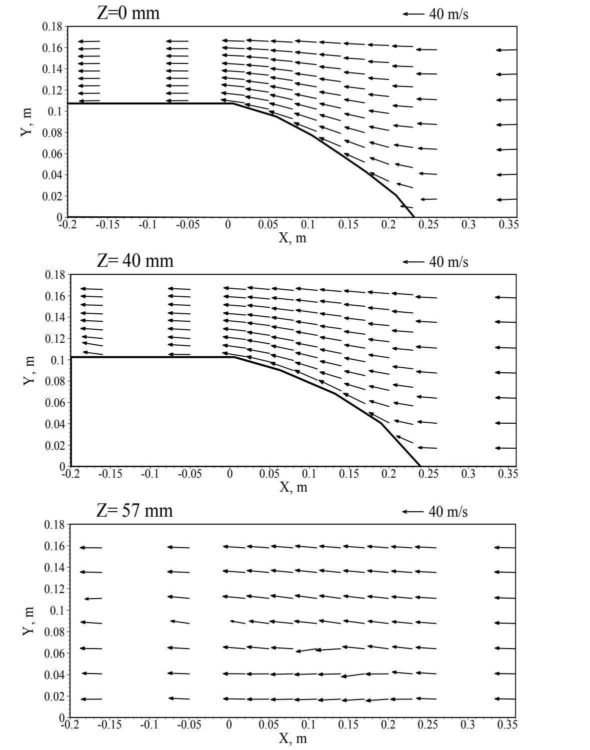


Figure 12. Velocity vectors over the New Model Front at different Z values at 40 m/s using X-Probe

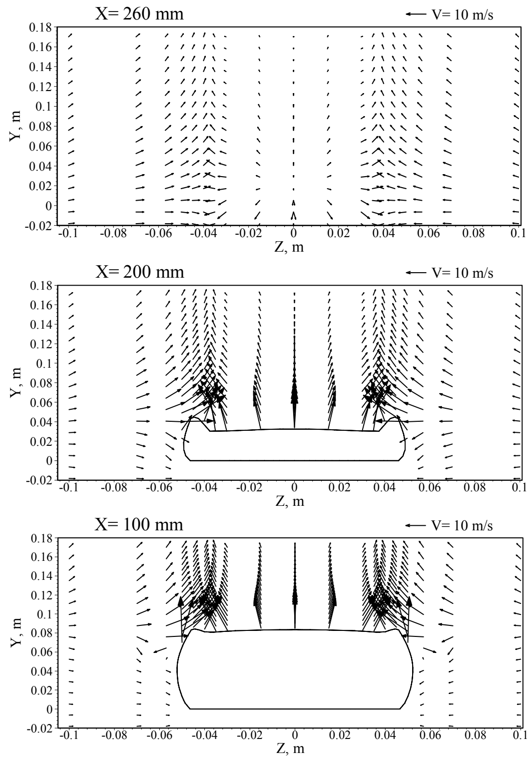


Figure 13. Velocity vectors over the New Train Front Model at 40 m/s flow velocity with different X values using X-Probe.

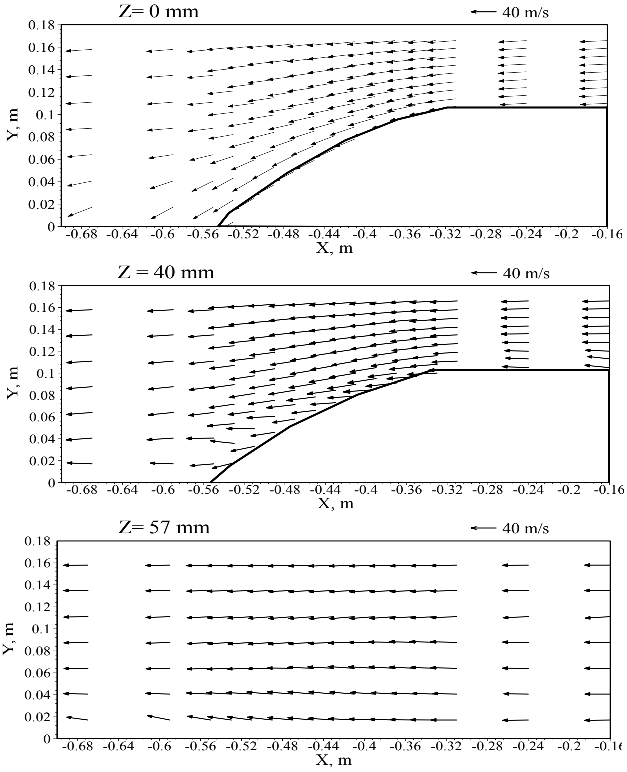


Figure 14. Velocity vectors over the New Model Rear at 40 m/s flow velocity with different Z values using X-Probe.

Figure 15. shows the X-Probe velocity vectors over the new train model rear at different X planes; just behind train model X=-560, far from the model X=- 700 mm and far away from the model X=-800 mm. The results indicate that strong vortices were created downstream the train model rear and vanished far away behind it.

**CONCLUSION**

The surface pressure coefficient for the new finned train model (M1) is less than that of the original train model (M0) in the rear region, and is about the same in the front region, revealing wake modification in the new model case.

Flow visualization for both train models indicates that the flow field is generally smooth over the train body except on the train front and rear. Strong vortices are noticed in the wake area of both train models. However in the absence of guiding vanes, the secondary vortices are unstable; in case of fins they are much more stabilized and uniform.

Good agreements are obtained between the X-hotwire data and the PIV data for the flow pattern in the train model rear.

The Experimental results indicate that the drag coefficient for the new finned train model is less than the other model by 14% at 10 m/s and 7% at 40 m/s velocity.

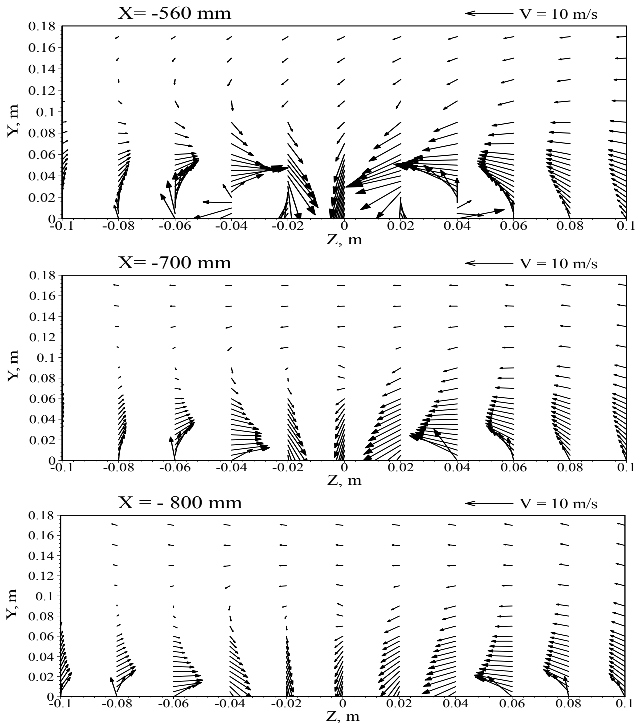


Figure 15. Velocity vectors over the New Model Rear at 40 m/s at different X values using X-Probe

**ACKNOWLEDGEMENT**

Thanks are due to Prof. Kohama Lab. Members; Assistant Professor Takuma Kato, Research Associate Satoshi Kikuchi, Technician Fukuo Ohta, Mr. Suzuki, and Mr. Yamabe for their assistance in conducting this work.

**REFERENCES**

1- Raghu S.R., Kim H.D. and Setoguchi "Aerodynamics of High-Speed Railway Train" Progress in Aerospace Sciences 38,469-514, 2002.
2- Willemsen E. "High Reynolds Number Wind-Tunnel Experiments on Trains" Journal of Wind Engineering and Industrial Aerodynamics, 69-71, 437-447, 1997.
3- M. I. Kamal "Experimental and Theoretical Investigation of the Flow around High Speed Trains" Ph. D. Thesis, Cairo University, Faculty of Engineering, Feb. 2006.
4- Ogawa T. and Fujii K. "Numerical Simulation of Compressible Flows induced by a train moving into a tunnel" Computational Fluid Dynamics Journal, Vol. 3, No. 1, 63-82, April 1994.
5- Schetz A.J. and Fuhs E.A." Handbook of Fluid Dynamics and Fluid Machinery" Vol. 3, Applications of Fluid Dynamics.
6- "Scanivalve for measuring multiple Pressures" Model J. Catalog, Scanivalve Corp., 1972.

 